# Pattern-search inversion for hypocenter location

Lejia Han, Joe Wong, and John C. Bancroft


## ABSTRACT

Pattern-search (PS) inversion on one-component (1C) recordings was used to locate hypocenter location, in contrast to our back-propagation analysis method for three-component (3C) microseismograms. The efficiency and associated accuracy of PS inversion was examined through its regression progress in four scenarios.


## INTRODUCTION

Microseismic monitoring is most likely conducted in borehole applications with triaxial sensors (Maxwell, 2001), by which the incident phase of propagation at each recording site can then be approximated with a choice of polarization analysis methods. Hence propagation direction or polarization based methods are common for locating microseismic hypocenters, such as the ts-tp method (Saari, 1991) or the back-propagation method (Han et al, 2010).

If microseismic monitoring does not involve triaxial recording, as surface microseismic surveys are usually 1C (Duncan, 2005; Lakings et al., 2006; Chambers et al., 2008), incident phases of propagation cannot be obtained by any direction or polarization analysis method, and hence we have to return to a conventional imaging methodology like inversion or migration in such situations.

In contrast to our propagation direction based method that demands triaxial recording, i.e. back-propagation analysis on 3C microseismograms, the pattern-search (PS) inversion method is used and evaluated for its ability and efficiency to locate microseismicity on 1C microseismograms.

Test data are obtained as simulated results from a few well and surface monitoring scenarios created in MATLAB software, for a six-fold horizontally layered velocity model, which is calibrated, first of all, by a PS inversion as well.

## ABOUT THE PS INVERSION ALGORITHM

The PS algorithm (Hookie and Jeeves, 1960) was first introduced as an unconstrained search technique that does not explicitly use derivatives. Kolda et al. (2003) provided a valuable review and feedback about this optimization algorithm after decades of usage and evaluation, along with a broad class of methods to handle bound constraints and linear/nonlinear constraints.

The PS algorithm was first attempted in CREWES by Bland and Hogan (2005) to locate microseismic hypocenters in a 3D velocity field. A later investigation in a 2D velocity field emerged in CREWES recently as well (Wong et al., 2010). In this paper, the latest tests and results in a horizontally layered velocity model will be illustrated with a variety of geophysical scenarios.

The earlier experiment in CREWES has compared three optimization algorithms from two categories, i.e. a genetic algorithm (GA) and a pattern-search (PS) algorithm, both from the direct search category, and a Levenberg-Marquardt (LM) algorithm from the gradient-based category, for their efficiency and accuracy in solving problems related to microseismic monitoring and hypocenter location. It was concluded that the gradient-based inversion methods such as the LM algorithm can easily be trapped in local minima even when only two parameters are to be found. If more parameters are required, for example, in calibrating a multiple layered velocity model, the likelihood for the existence of more local minima, saddle points, or long narrow data valleys is increased. Using a gradient-based method to find a global minimum in such cases is likely to end as a frustrating experience. Alternatives to gradient-based methods exist in the form of sophisticated global search techniques such as the GA or PS method (Torczon, 1997; Vose, 1999; Kolda et al., 2003; articles in wikipedia.org), with the following advantages:

- They are often faster.
- They are much less prone to being trapped in local minima.
- They require no calculation of partial derivatives of the objective function.
- Available implementations of such algorithms, for example, by MATLAB software, are easy to use.

Based on the simulated geophysical scenarios and testing results (Wong et al., 2010), further conclusions include that PS performed more efficiently than GA, taking only about 1/10 the number of objective function evaluations to produce smaller misfit errors; PS performed well even if the initial guess for the velocities was far from the true values, and converged to the true values regardless of whether the lower or the upper bounds were used as starting values.

In general, an inversion algorithm is expected to produce the unknown parameters through a series of iterative calculations that decrease the objective or misfit function gradually and/or quickly depending on the searching strategy that characterizes the inversion algorithm, until the final set of parameters that meets the predefined criterion as the local or global minimum.

In this report, the recommend PS inversion algorithm is to be examined through velocity calibration and hypocenter location on simulated data through a horizontally layered velocity model by various recording geometries.

The inversion procedure, by either gradient based algorithms or direction search algorithms, for calibrating a velocity model and locating hypocenters within geophysical scenarios simulated in this chapter, always involves the general steps, as described in the Appendix.

## FORWARD MODELLING

For all simulated scenarios later in this paper, forward modelling, employing Snell's Law and ray-tracing, is used to generate a set of first-arrival times as a function of depth in either a layered velocity model or a set of velocity estimates with sufficient take-off angles from either a perforation shot or a microseismic hypocenter or estimate to geophone arrays deployed in wells or on the surface. More specifically, the PS inversion

procedure will obtain both "observed" arrival times and "modeled" arrival times by P wave ray-tracing through an earth model of six horizontal layers with velocities and boundary depths, as defined and shown in Figure 1(a) for well monitoring scenarios, and Figure 2(a) for a surface monitoring scenario. By "observed" is meant that the arrival times are obtained by forward modelling through the established or pre-defined earth model, while "modeled" (or "calculated") means the arrival times from a series of iterative search calculations starting from the initial model assumption by a chosen inversion technique such as the PS inversion, until some criterion is met.

In all testing and experiments hereafter, it should be known that the reduced arrival time was used instead of the actual time of occurrence t0 of a microseismic event. The former is usually unknown in real-world microseismic monitoring and is an extra parameter that has to be found by additional work. Thus, the reduced arrival times tobs(i) – min(tobs(i)) and tcal(i) – min(tcal(i)) are to be used for the PS inversion and evaluation in all applied scenarios later in this chapter. This simple adjustment means that arrival-time moveouts rather than absolute arrival times are the basis for calibrating the velocity model and locating the hypocenter as well, eliminating the need to know the event time t0. However, the moveout times must be large enough in all case simulations so that they exceed any time-picking errors, and the angles subtended by the geophone arrays relative to the source should span a range of ±20 degrees or more, in order to contain sufficient geometric information for locating the hypocenter.

Another convention that simplified all testing and experiments in this paper is that the cylindrical coordinates (rs, zs) are used, and horizontal coordinates (xs, ys) or azimuth angles are ignored due to the limitation of one-component recordings.

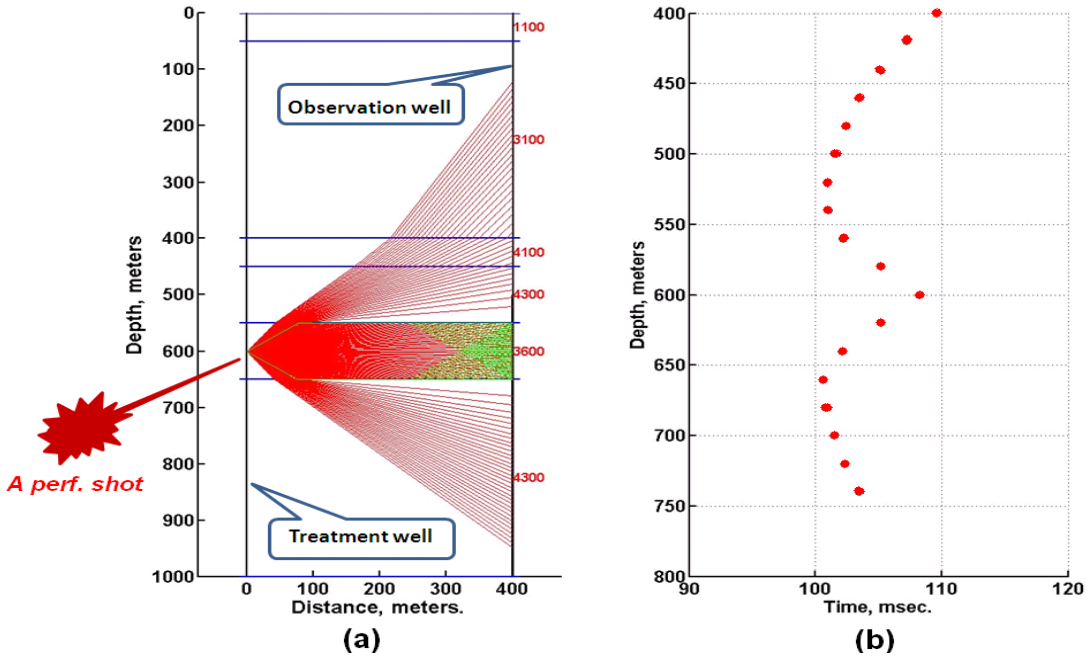


FIG.1 Forward modeling and data simulation for a well. (a) Ray-tracing (red rays) from a perforation shot to an observation well, with green rays denoting head wave arrivals through the low-velocity zone. (b) The associated first arrival times.

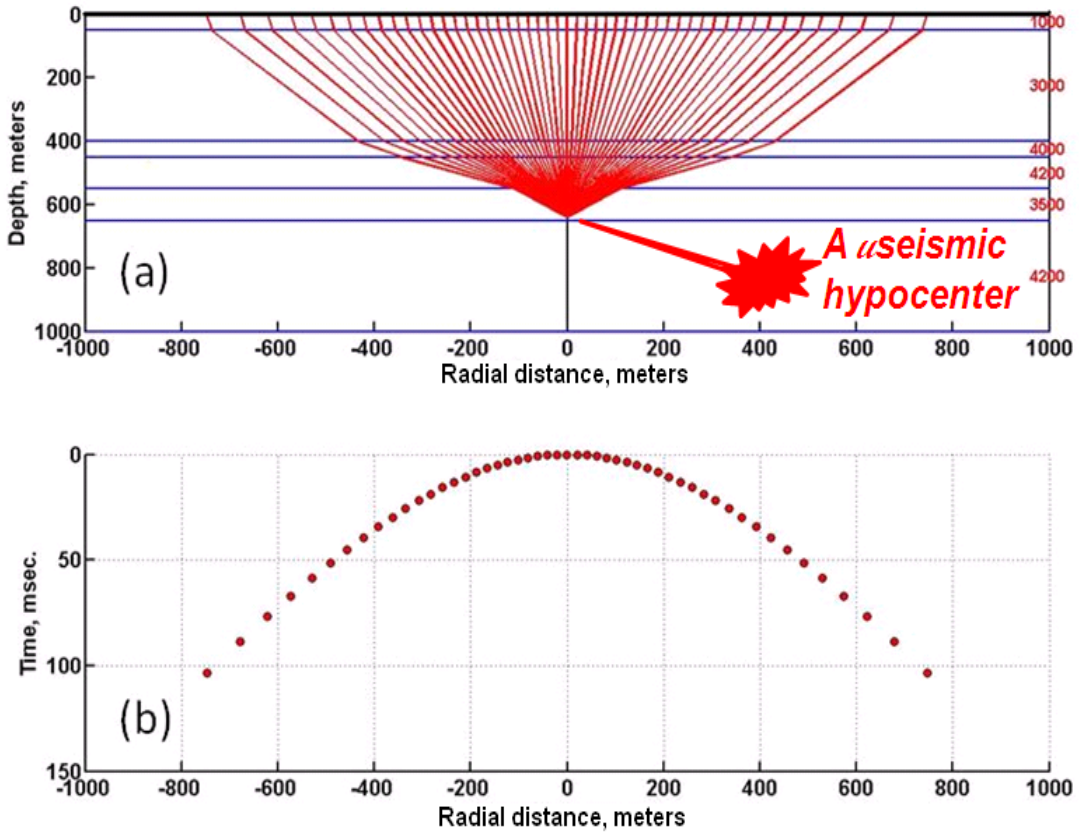


FIG.2 Forward modeling and data simulation for a surface survey. (a) Ray-tracing from a deep microseismic source to a surface geophone array. (b) The associated first arrival times.

## VELOCITY CALIBRATION

In the analysis of a real-world microseismic dataset, an essential first step is the calibration of the velocity model with boundary depths which are usually known, for example, from gamma-ray logs.

The velocity calibration here is first through simulating a casing perforation shot in a treatment well, and then ray tracing through a layered model to an array of 18 geophones separated by 20 m in an observation well, as shown in Figure 2(a). The unknown velocities are then to be calibrated by PS inversion with the "observed" arrival times, the geophone coordinates, and the shooting source coordinates.

The PS inversion procedure uses the objective function of equation (1) for velocity calibration and generates a series of the root-mean-square (RMS) differences between observed arrival times and modeled (or calculated) arrival times at an iteration of the PS searching or regressing series. The initial assumption of the layered model velocities is required to launch an inversion procedure.

The initial guess of [v1, v2, v3, v4, v5, v6], representing the six-layer model velocities from the top to the bottom as shown in Figure 7.2(a), is set to [1000, 2000, 2000, 2000,

2000, 2000] m/s. Since the overburden velocity played no role in determining arrival times for this particular source-receiver geometry, it was fixed by setting its lower and upper bounds at 1000 m/s.

To accelerate the searching progress, reasonable lower and upper bounds for the velocities [v1, v2, v3, v4, v5, v6] were set at [1000, 2000, 2000, 2000, 2000, 2000] and [1000, 6000, 6000, 6000, 6000, 6000] m/s, respectively. Table 1 summarizes the calibrating progress by the PS inversion procedure (implemented and provided within MATLAB).

The last column in Table 1 shows the arrival-time misfits measured by the RMS error and the associated iterations in the first column including the evaluation counts of the objective function within parentheses. It can be observed that the velocity set shown in each row gradually converges to the true velocity values shown in the bottom row as the number of iterations increases from zero (i.e., the initial guess), to 10, 20, until 40 where the RMS misfit is down to 0.45 ms, from 16.5 ms at the initial guess. Figure 3 illustrates this progress with the velocity profiles and the associated reduced arrival times.

Table 1: Summary of velocity calibration using PS inversion

| Iterations (iter) | Evaluations (iter2) | $v_1$ (m/s) | $v_2$ (m/s) | $v_3$ (m/s) | $v_4$ (m/s) | $v_5$ (m/s) | $v_6$ (m/s) | Error (ms) |
|---|---|---|---|---|---|---|---|---|
| 0 | 0 | 1000 | 2000 | 2000 | 2000 | 2000 | 2000 | 16.5 |
| 10 | 8 | 1012.6 | 4030.9 | 2107.1 | 3040.2 | 4509.3 | 4129.9 | 5.14 |
| 20 | 58 | 1109.8 | 5010.7 | 3059.9 | 4103.2 | 4089.2 | 4035.6 | 1.66 |
| 40 | 229 | 1050.6 | 2510.9 | 4250.3 | 4125.7 | 3509.9 | 4125.1 | 0.45 |
| True | Model: | 1000 | 3000 | 4000 | 4200 | 3500 | 4200 | 0 |

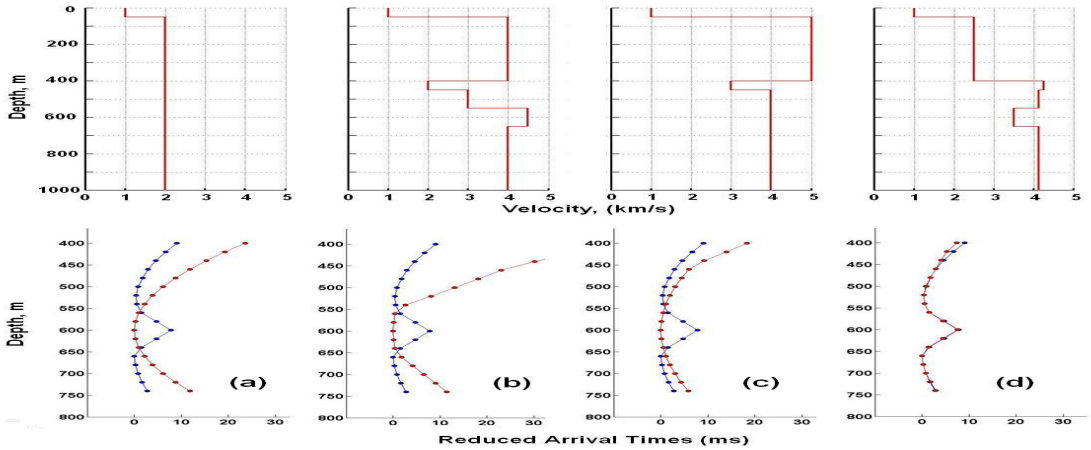


FIG.3 The velocity profiles (top panel) and the arrival-time misfits (bottom panel) between observed (red dots) and calculated (blue dots) times resulted from (a) the initial guess, (b) 10 iterations, (c) 20 iterations, and (d) 40 iterations, using PS inversion for calibrating velocities.

It can be observed that the initial velocity profile on Figure 3(a) evolved to the final profile on Figure 3(d), where the calculated arrival times gave an almost perfect fit to the observed arrival times.

The above inversion procedure demonstrates that the PS searching algorithm converges quickly in this simulated scenario of velocity calibration.

## HYPOCENTER LOCATION

There will be three simulated scenarios for locating hypocenters by PS inversion. In the first case, a single microseism is monitored from a single vertical well; the second case is comprised of three shallow vertical wells, and in the third case, surface geophone arrays take the roles of the wells of case two.

### Hypocenter location-estimation with a single vertical well

The geophysical scenario used here for the PS inversion utilization and evaluation as shown in Figure 4, monitors a microseism located in the velocity model of Figure 1 at (xs, ys, zs) = (10 m, 0 m, 620 m). Arrival times are obtained at 18 geophones separated by 20 m in a vertical observation well with the topmost geophone at a depth of 400 m, assuming the velocity model shown in Figure 1. Table 2 summarizes the locating progress using PS inversion with the initial location assumption (xs, ys, zs) = (100 m, 0 m, 800 m).

Table 2: Summary of hypocenter location using PS inversion (for a single vertical well)

| Iterations (iter) | Evaluations (iter2) | $x_s$ (m) | $y_s$ (m) | $z_s$ (m) | RMS error (ms) |
|---|---|---|---|---|---|
| 0 | 0 | 100 | 0 | 800 | 8.09 |
| 20 | 56 | 40.7 | 0 | 614.4 | 0.64 |
| 40 | 115 | 19.3 | 0 | 623.0 | 0.30 |
| 60 | 186 | 9.9 | 0 | 619.8 | 0.02 |
| True | Location: | 10.0 | 0 | 620.0 | 0 |

It can be observed that, as the number of iterations increases, the location estimate's accuracy improves consistently, and after 60 iterations, with 186 evaluations of the objective function, the location estimate (xs, ys, zs) = (9.9 m, 0 m, 619.8 m) produced by this PS procedure is almost at the true location. The PS performance can also be overviewed through the RMS misfits of the reduced arrival times between the observed and calculated times, as illustrated in Figure 4.

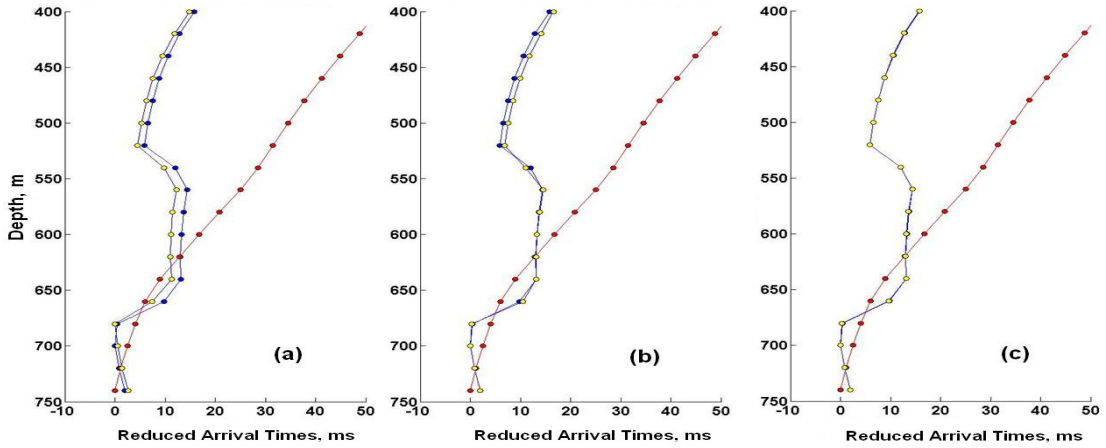


FIG.4 The arrival-time misfits between observed (blue dots) and calculated (yellow dots) times resulting from (a)20 iterations, (b)40 iterations, and (c)60 iterations, from the initial assumption (red dots) within one vertical well.

After 60 iterations, as shown in Figure 4(c), the calculated reduced arrival times (yellow dots) matched the observed reduced arrival times (blue dots) almost perfectly. A big regression progress was obtained even at a very early time, e.g. after 20 iterations, even though the initial assumption deviated considerably from the true velocities.

**Hypocenter location-estimation with three shallow vertical wells**

Placement of clamped 3C geophone arrays in deep observation wells is difficult, expensive, and limited by the availability of, and access to, deep wells. In some situations, microseismic monitoring can be done effectively by using inexpensive hydrophone arrays in shallow wells that penetrate beneath the attenuating overburden and near-surface rocks. Since shallow wells (less than 400 m deep) are inexpensive, several can be drilled in locations that straddle the anticipated fracture zones near the treatment well. The well locations can be designed to give adequate angular coverage and to enable accurate hypocenter location through the inversion of event arrival times.

Figure 5 shows three arrays of 12 hydrophones or geophones deployed in three shallow vertical wells. For each array, the depth of the topmost receiver is 100 m, and the receiver spacing is 20 m. The surface locations of the three observation wells are (xw, yw) = (500 m, 500 m), (200 m, -500 m), and (-500 m, 300 m). A set of "observed" arrival times was generated assuming the velocity structure on Figure 1. The source coordinates then were estimated by inverting the reduced arrival times with the PS algorithm.

Table 3 summarizes the searching or regression progress for the hypocenter location-estimation with three shallow vertical geophone arrays.

It can be observed from the above table that the final product took 31 iterations and 91 evaluations of the objective function, which means even fewer steps than the cost for the final product in the previous single well case. Figure 5 plots the observed and calculated reduced arrival times at various regressing stages in this PS inversion procedure.

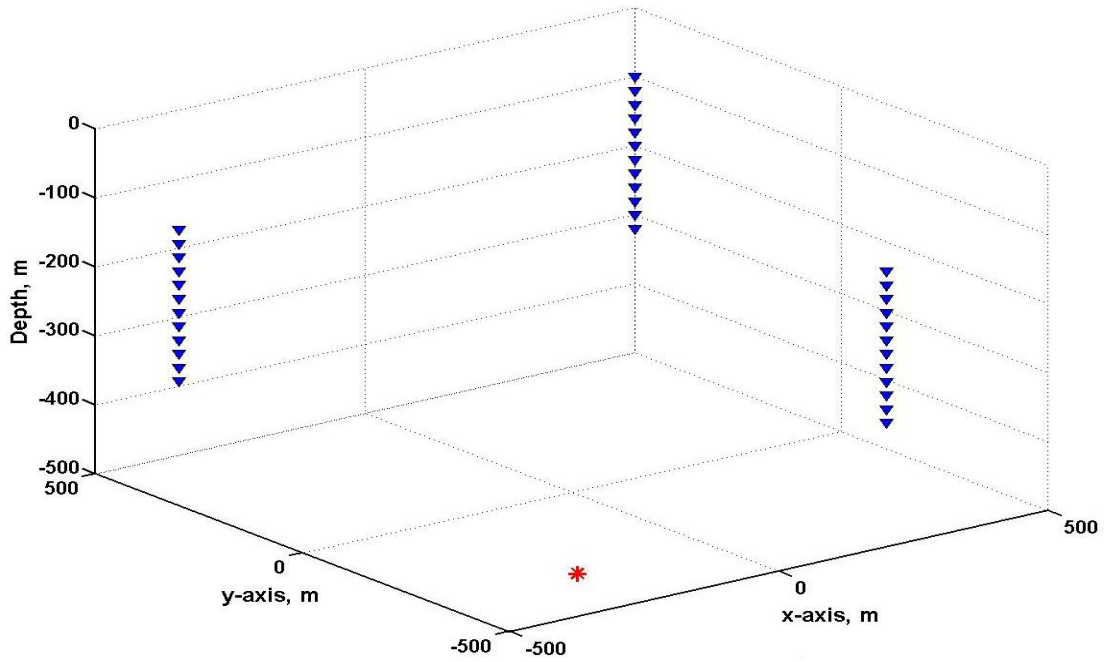


FIG.5 Three vertical geophone arrays (blue triangles) are straddling the microseismic source (the red star).

Table 3: Summary of hypocenter location using PS inversion with three shallow vertical wells

| Iterations (iter) | Evaluations (iter2) | $x_s$ (m) | $y_s$ (m) | $z_s$ (m) | RMS error (ms) |
|---|---|---|---|---|---|
| 0 | 0 | 100 | 100 | 800 | 20.12 |
| 11 | 12 | 50.1 | 12.9 | 600.3 | 6.38 |
| 21 | 30 | 26.7 | 6.1 | 603.9 | 0.30 |
| 31 | 91 | 10.8 | 2.3 | 607.5 | 0.15 |
| True | Location: | 10 | 0 | 620 | 0 |

The right panel corresponds to the slowest fitting-in well, while the other two panels correspond to better fitting wells in spite of worse fits at the initial time. Nevertheless, the overall fittings from the three wells are satisfactory, and hence the location estimate is acceptable.

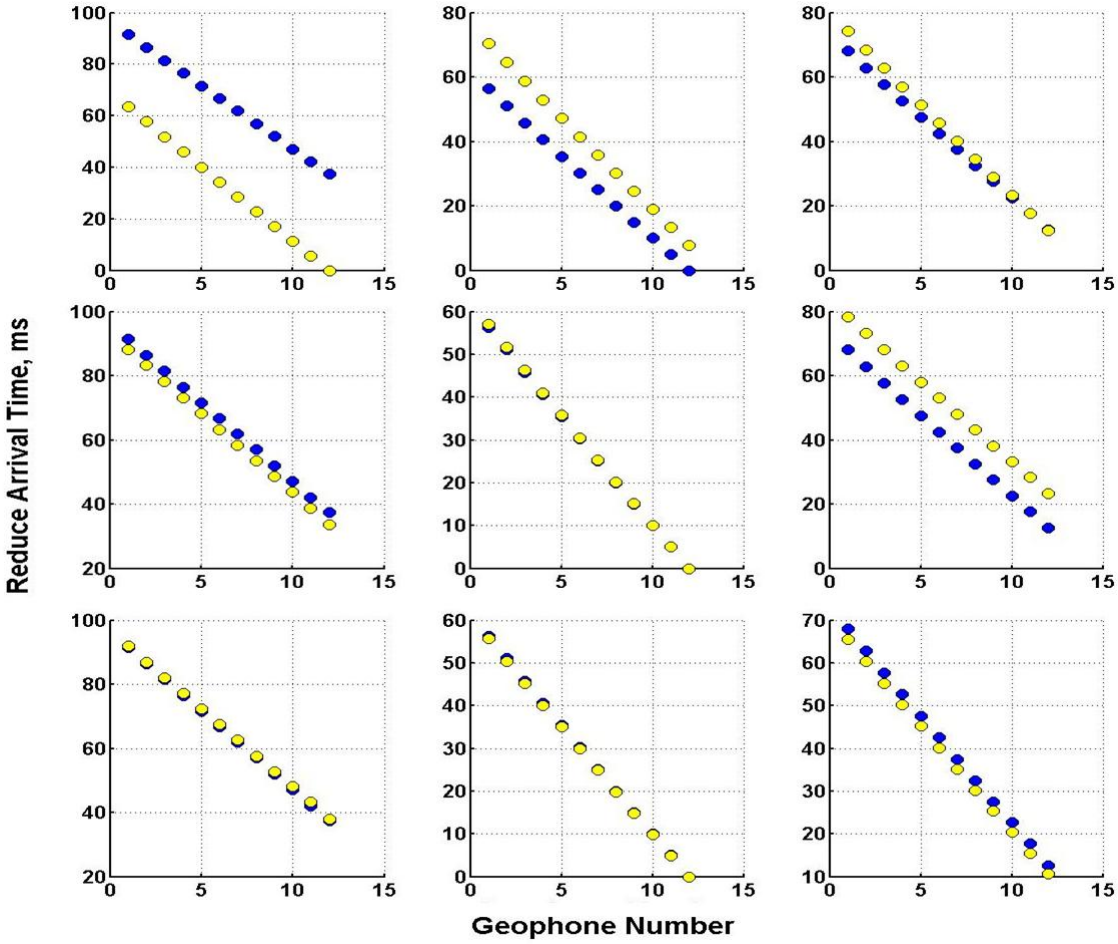


FIG.6 The left, middle, and right panels represent the arrival-times misfits between observed times (blue dots) and calculated times (yellow) resulting from (a) initial guess, (b) 11 iterations, and (c) 31 iterations, with three vertical wells.

## Hypocenter location-estimation with surface geophone arrays

Surface geophone arrays are often used for monitoring microseismic events produced by the hydraulic fracture stimulation of a reservoir (Duncan, 2005; Lakings et al., 2006; Chambers et al., 2008). In a real-world situation, hundreds of geophones may be deployed, either along lines radiating from the treatment well, or on a rectangular grid. A simplified recording scenario is shown on Figure 7, which displays a surface array of a total of 60 geophones (blue triangles), spanning distances of about 600 m in both the x and y directions.

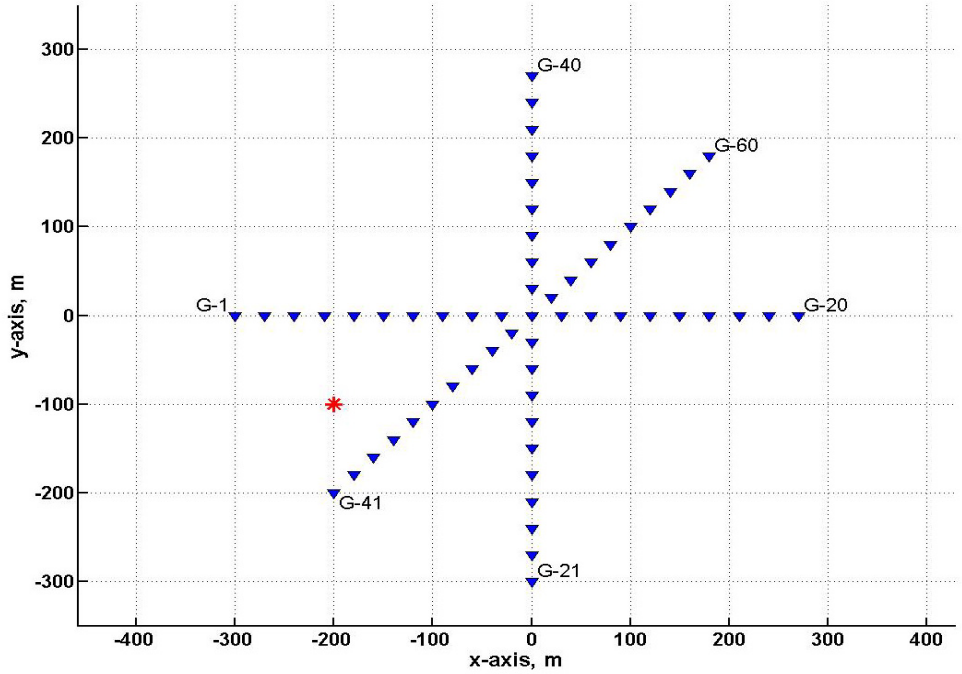


FIG.7 Map view of surface geophone arrays (blue triangles) monitoring a single microseism (the red star) at a depth of 640m.

The geophones are approximately centered about the treatment well. A microseismic source located in the vicinity of the well at a depth of 640 m is shown in red. The "observed" arrival times were generated by ray tracing through the layered velocity structure shown on Figure 2(a). The source coordinates were then estimated by inverting the reduced arrival times using the PS algorithm. The locating progress using PS inversion for this surface monitoring scenario is summarized in Table 4.

Table 4: Summary of PS inversion for hypocenter location with surface geophone arrays

| Iterations (iter) | Evaluations (iter2) | $x_s$ (m) | $y_s$ (m) | $z_s$ (m) | RMS error (ms) |
|---|---|---|---|---|---|
| 0 | 0 | 0 | 0 | 800 | 22.1 |
| 11 | 38 | -230 | -80 | 640 | 2.36 |
| 51 | 200 | -222.5 | -110 | 672.5 | 0.90 |
| 101 | 459 | -207.5 | -102.5 | 626.25 | 0.30 |
| True | Location: | -200 | -100 | 640 | 0 |

As shown in Figure 8, even with the initial assumption (red dots) far deviated from the observed arrival-times (blue dots), the calculated times (yellow dots) fit well even at the

earliest stage of progress shown in Figure 8(a), with the RMS error down to 2.36 ms from 22.1 ms with the initial velocity-model assumption.

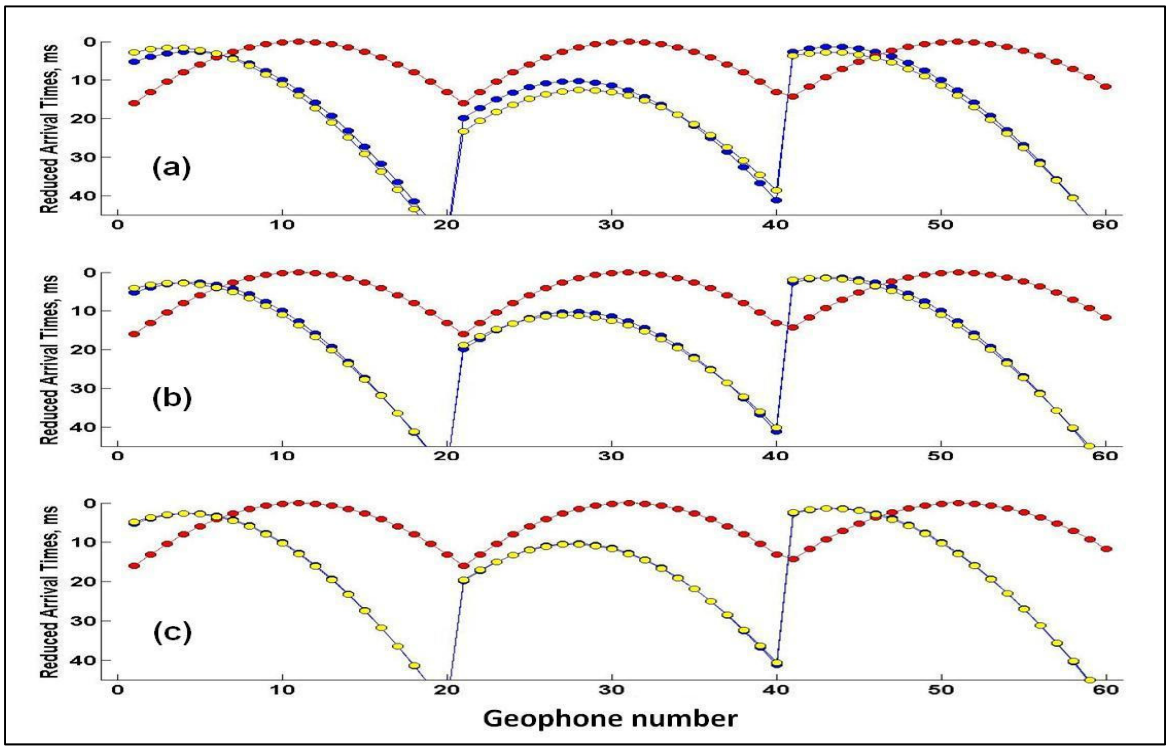


FIG.8 The arrival-time misfits between observed times (blue dots) and calculated times (yellow dots) resulting from (a) 11 iterations, (b) 51 iterations, and (c) 101 iterations, from the initial assumption (red dots) with surface geophone arrays.

The RMS error then quickly dropped from 0.90 ms at 51 iterations to 0.30 ms at 101 iterations, as shown in Table 4. This indicates that the PS inversion converges consistently and quickly even when the initial assumptions are far from the truth.

It can be observed from Table 4, by cross-checking the PS inversion progresses from three microseismic monitoring scenarios, that the final location estimate was produced after 101 iterations with an RMS error of 0.30 ms, as illustrated in Figure 8(c), where the modeled arrivals fit the observed times well. However, the computing cost took 459 evaluations of the objective function for the final set of location coordinates, which is much more than 115 evaluations at 40 iterations and 91 evaluations at 31 iterations, with the associated RMS errors at 0.30 ms and 0.15 ms respectively for the two well scenarios in Table 2 and Table 3. This observation has also been collected in Table 5.

Table 5: Cross-evaluation of PS inversion progress in all applications for hypocenter location

| **Observations** *(1C microseismograms)* | *RMS error (ms)* | **Iterations** *(iter)* | **Evaluations** *(iter2)* |
|---|---|---|---|
| **In a single vertical well** | **0.30** | **40** | **115** |
| **In three shallow vertical wells** | **0.30** | **21** | **30** |
| **On surface** | **0.30** | **101** | **459** |

## SUMMARY

With one-component recordings, microseismic monitoring and hypocenter location has to employ a conventional imaging method. In such situations, we employed the pattern-search inversion algorithm and conducted the testing in three seismic surveys of a six-layered horizontal velocity model, in wells and on the surface. The efficiency of the PS inversion is demonstrated most favorably by its regression cost on P-wave observations in three shallow vertical wells requiring only 51 function evaluations over in the single vertical well's 155, and the surface array's 600 function evaluations to arrive at an equivalent RMS error of 0.30 milliseconds.

## APPENDIX

The general steps for an inversion method to calibrate a velocity model or locate a hypocenter:

1. Define an objective function $\boldsymbol{rms\_err}$ equal to the root-mean-square error between $n$ observed arrival times $\boldsymbol{t_{obs}}$ and $n$ calculated or modeled arrival times $\boldsymbol{t_{cal}}$ for calibrating model velocity $(v_1, v_2, v_3, v_4, v_5, v_6 t_{obs})$ and locating hypocenters $(\boldsymbol{x_s}, \boldsymbol{y_s}, \boldsymbol{z_s})$ respectively with:

$$\boldsymbol{rms\_err}(\boldsymbol{v_1}, \boldsymbol{v_2}, \boldsymbol{v_3}, \boldsymbol{v_4}, \boldsymbol{v_5}, \boldsymbol{v_6}) = \sqrt{\sum_{i=1}^{n} [\boldsymbol{t_{obs}}(\boldsymbol{i}) - \boldsymbol{t_{cal}}(\boldsymbol{i}, \boldsymbol{v_1}, \boldsymbol{v_2}, \boldsymbol{v_3}, \boldsymbol{v_4}, \boldsymbol{v_5}, \boldsymbol{v_6})]^2} \quad (1)$$

and

$$\boldsymbol{rms\_err}(\boldsymbol{x_s}, \boldsymbol{y_s}, \boldsymbol{z_s}) = \sqrt{\sum_{i=1}^{n} [\boldsymbol{t_{obs}}(\boldsymbol{i}) - \boldsymbol{t_{cal}}(\boldsymbol{i}, \boldsymbol{x_s}, \boldsymbol{y_s}, \boldsymbol{z_s})]^2}. \quad (2)$$

2. Determine the experimental error as the threshold value ***exp_err***, and the maximum number of searching iterations ***iter_max*** and associated evaluations of the objective function ***iter2max***. Set the iteration counter ***iter*** and the objective function counter ***iter2*** to 1.

3. Make an initial guess of the model parameters $(\boldsymbol{v_1, v_2, v_3, v_4, v_5, v_6})$ or the hypocenter location coordinates $(\boldsymbol{x_s, y_s, z_s})$.

4. Calculate $\boldsymbol{t_{cal}}$ for i=1 to n by forward modeling through the layered velocity model.
5. Calculate ***rms_err*** according to the two objective functions stated above.
6. Go to Step 13 if ***rms_err*** is less than ***exp_err***.
7. Use the searching strategy at this stage such as the current residuals and/or the objective functions to estimate corrections $\boldsymbol{(\Delta v_1, \Delta v_2, \Delta v_3, \Delta v_4, \Delta v_5, \Delta v_6)}$ or ($\boldsymbol{\Delta x_s}$, $\boldsymbol{\Delta y_s}$, $\boldsymbol{\Delta z_s}$).
8. Update the respective parameters $\boldsymbol{(v_1 = v_1 + \Delta v_1,\ v_2 = v_2 + \Delta v_2,\ v_3 = v_3 + \Delta v_3,\ v_4 = v_4 + \Delta v_4,\ v_5 = v_5 + \Delta v_5,\ v_6 = v_6 + \Delta v_6)}$ or ($x_s = x_s + \Delta x_s$, $y_s = y_s + \Delta y_s$, $z_s = z_s + \Delta z_s$).

9. Calculate $t_{cal}$ and ***rms_err***.
10. Go to 13 if ***rms_err*** is less than ***exp_err***.
11. If the current ***rms_err*** is greater than the last ***rms_err***, then use the searching strategy at this stage to re-correct:

    a. Reset to the latest calculated results
        i. $\boldsymbol{(v_1, v_2, v_3, v_4, v_5, v_6) = (v_1 = v_1 - \Delta v_1,\ v_2 = v_2 - \Delta v_2,\ v_3 = v_3 - \Delta v_3,\ v_4 = v_4 - \Delta v_4,\ v_5 = v_5 - \Delta v_5,\ v_6 = v_6 - \Delta v_6)}$ or
        ii. $(x_s, y_s, z_s) = (x_s = x_s - \Delta x_s,\ y_s = y_s - \Delta y_s,\ z_s = z_s - \Delta z_s)$;

    b. Correct according to results from the re-searching algorithm
        i. $\boldsymbol{(\Delta v_1,\ \Delta v_2,\ \Delta v_3,\ \Delta v_4,\ \Delta v_5,\ \Delta v_6) = (a_1 \Delta v_1,\ a_2 \Delta v_2,\ a_3 \Delta v_3,\ a_4 \Delta v_4,\ a_5 \Delta v_5,\ a_6 \Delta v_6)}$ or
        ii. $\boldsymbol{(\Delta x_1,\ y_2,\ \Delta z_3) = (\beta_1 x_s,\ \beta_2 y_s,\ \beta_3 z_s)}$;

    c. Update the parameters
        i. $\boldsymbol{(v_1 = v_1 + \Delta v_1,\ v_2 = v_2 + \Delta v_2,\ v_3 = v_3 + \Delta v_3,\ v_4 = v_4 + \Delta v_4,\ v_5 = v_5 + \Delta v_5,\ v_6 = v_6 + \Delta v_6)}$ or
        ii. $(x_s = x_s + \Delta x_s,\ y_s = y_s + \Delta y_s,\ z_s = z_s + \Delta z_s)$;

    d. Calculate $t_{cal}$ and ***rms_err*** ;
    e. Go to step 13 if ***rms_err*** is less than ***exp_err***;
    f. Go to (b) if ***rms_err*** has increased;
    g. Set ***iter2*** = ***iter2***+1;
    h. Go to (a) if ***iter2*** <= ***iter2max***.
12. Increment ***iter*** = ***iter*** +1.
13. If ***iter*** < ***iter_max*** go to step 3.
14. Return the latest set of parameters.

The search strategy for step 7 and step 11 will characterize a particular direct search algorithm, and the searching efficiency will be evaluated in terms of iter as the number of search iterations and iter2 as the number of objective-function evaluations of the PS algorithm.

Coding effort, for testing the PS algorithm within all simulated geophysical scenarios in this chapter, was saved by the optimtool utility bundled in the MATLAB (2009) optimization toolkit, where many other sophisticated optimization algorithms have been implemented and provided with great flexibility to users and applications.

## ACKNOWLEDGEMENTS

The first author sincerely appreciates the tremendous time and advices on both technical discussions and English editing help from Dr. Rolf Maier.

The authors gratefully acknowledge the support of the CREWES sponsors.

## REFERENCES

Bancroft, J. C. (2009). Estimating the location of a microseismic event using a vertical array of receivers. CREWES Report, 21 , pp. 6.1-6.10.

Bancroft, J. C., Wong, J., and Han, L. (2010). Sensitivity measurements for locating microseismic events. CSEG Recorder, 35 , 27-36.

Bland, H. C., and Hogan, C. (2005). A hypocenter location method for microseismicity in complex regions. CREWES Research Report 17 , pp. 18.1-18.14.

Chambers, K., Brandsberg-Dahl, S., Kendall, J. M., and Rueda, J. (2008). Testing the ability of surface arrays to locate microseismicity. 78th Ann. Int. Meeting, SEG Expanded Abstracts, (pp. 1436-1439).

Lakings, J. D., Duncan, P. M., Neale, C., and Theiner, T. (2006). Surface based microseismic monitoring of a hydraulic fracture well stimulation in the Barnett shale. 76th Ann. Int. Meeting, SEG Expanded Abstracts, (pp. 605-67).

Maxwell, S. C., and Urbancic, T. I. (2001). The role of passive microseismic monitoring in the instrumented oilfield. The Leading Edge, 20 , 636-639.